Spray Characterization of Gas-to-Liquid Synthetic Aviation Fuels

K. Kumaran, Reza Sadr*
Mechanical Engineering Program, Texas A&M University at Qatar, Qatar
kumaran.kannaiyan@qatar.tamu.edu and reza.sadr@qatar.tamu.edu

Abstract

Development of alternative aviation (jet) fuels is gaining importance in recent years to meet growing energy demand of the world and to reduce the environmental impact of aviation fuel combustion. Alternative fuels need to match the energy density as that of the conventional fuels and need to possess vital qualities such as rapid atomization and vaporization, quick re-ignition at high altitude and acceptable emission level. Gas-to-Liquid (GtL) synthetic paraffinic kerosene obtained from Fischer-Tropsch synthesis has grabbed global attention for its cleaner combustion characteristics due to the near absence of aromatics and Sulphur content in the fuel composition. Characterizing the atomization of the alternative liquid fuels is necessary as it affects evaporation process and mixing with air which, in turn affect combustion and emission characteristics of the fuel. As a part of an ongoing joint research effort between Texas A&M University at Qatar (TAMUQ), Rolls-Royce (UK), and German Aerospace Laboratory (DLR), an experimental facility was built at TAMUQ to study the spray characteristics of different GtL blends. The main objective of this work is to investigate the influence of the change in fuel composition on the spray characteristics at different injection pressures using a pressure (simplex) nozzle. The GtL blends used in this work consist of varying degree of cyclic carbon content and iso-to-normal paraffin ratio that fit in between the commercial GtL kerosene and the commercial paraffinic solvents. A planar optical diagnostic technique, Global Sizing Velocimetry is used in this work to study the spray characteristics, such as droplet size, distribution and velocity, of three different GtL blends and the results are compared with that of the conventional Jet A-1 fuel. The droplet size distributions highlight the influence of fuel composition on the mean droplet size, distribution and spray structure among different blends.

Introduction

The depletion of fossil fuels and stringent emission norms has prompted the need for alternative aviation fuel source. Synthetic fuels manufactured from different feedstock's using Fischer-Tropsch (FT) process have grabbed the global attention due to their cleanliness. Synthetic paraffinic kerosene (SPK) produced from natural gas using FT process is identified as one of the alternative fuel that can be used without any modification to the existing design of the gas turbine combustors. However, to optimize the design of combustors for alternative fuel to extract the maximum potential of alternative fuels requires detailed investigation of atomization, mixing and combustion process. A brief summary of the literature pertaining to synthetic fuels for aviation industry is presented next.

Le Clercq et al., [1] numerically investigated the impact of Fischer-Tropsch (FT) synthesized, drop-in fuels on the spray and combustion performance in a rich-burn, quick-quench, lean-burn (RQL) combustor. In their study, fuels such as JetA-1, Sasol Fully Synthetic Jet Fuel (FSJF) (a blend of F-T SPK and tar coal derived hydrocarbons) and 100% Gas-to-Liquid (GtL) were represented by multi-component surrogate fuels. Finite-rate chemistry and an assumed-PDF approach for turbulence-chemistry interaction were adopted. Same reaction kinetics model was used for all the fuels. Computational results were reported to show a qualitatively, identical temperature and OH* fields. In addition, the soot precursor (acetylene) was also reported to show a considerable difference among the fuels which was attributed to the reaction kinetics used. Kahandawala et al., [2] experimentally investigated the effect of fuel composition on the ignition and emission characteristics. They studied the ignition time delay, soot production and polycyclic aromatic hydrocarbons (PAHs) of the surrogate and actual, synthetic (aka S8), synthesized from natural gas through FT process by syntroleum corporation and jet (JP-8) fuels. S8 is comprised of 82% iso-paraffins and 18% n-paraffin's. It was reported that the absence of aromatics in synthetic jet fuels slow the molecular growth to higher ringed PAHs which in turn lead to lower soot production. It was concluded that the fuel chemical structure has a significant higher impact on emissions than on chemical ignition delay.

Gokulakrishnan et al., [3] investigated the ignition characteristics of F-T syn jet fuel, S8 which consists of about 90% of paraffins (of which 80% is iso-paraffins and 20% is n-paraffins). They used a surrogate which included n-decane and iso-octane. From their experimental results of ignition delay it was indicated that the presence of iso-paraffins could have favorable impact on the operating conditions of the engine. Corporan et al., [4] reported a dramatic reduction in the particle concentrations (emission) and mean size with neat F-T (natural gas

derived) and syn jet fuel blend JP-8 when compared with JP-8 alone. They carried out the experiments in a T63 turboshaft engine. In T63 engine, operation at lower temperature (i.e., idle) showed significantly reduction in particulate matter (PM) with synjet when compared to JP-8 than operating T63 at higher temperature (i.e., cruise). Most of the above studies were focused on the combustion and emission characteristics. However, precursors of combustion process like atomization, evaporation and mixing plays a major role on the combustion process [5]. This emphasizes the need for detailed investigation of combustion precursors for synthetic jet fuels. Yao et al., [6] investigated the effect of viscosity on the instability of sprays in a swirl atomizer using a high speed video camera. They used varying concentrations of Glycerol-water mixtures to vary the viscosity. It was reported that viscosity had a significant effect on the spray cone angle and the breakup process.

In the past a vast majority of work on synthetic fuels was done in relation to alternate diesel engines and a large number of them reported a detailed investigation of the macro and micro spray characteristics for diesel engines. Recently, synthetic fuels have been considered as a good alternative aviation fuel. Since emission is the key driver of the engine development research, many investigations have been carried out to study the implication of alternate synthetic jet fuels on the combustion and emission characteristics in gas turbine combustors [7, 8] using a well understood atomizer for spray performance [5]. All these investigation clearly highlight the importance of synthetic jet fuel on the combustion and emission characteristics. However, the effect of synthetic fuel composition on the spray characteristics has hitherto been reported in the literature. This underscores the importance and the need for the characterization of the synthetic jet fuels derived using FT process.

In this work, the role of fuel composition on the spray characteristics has been investigated by using three different GtL-like fuel blends at three injection pressures using a simplex nozzle. The mean droplet diameter, size distributions and velocities are determined using the global sizing velocimetry (GSV) [9]. In addition, the spray cone shape is also qualitatively studied using a high speed camera.

Experimental Facility and methodology

Figure 1 shows the optically accessible spray experimental facility developed at TAMUQ for this work. The experimental facility consists of three modules namely, pump, spray chamber and optics module. In the pump module, the fuel is supplied from a supply tank to the pump through an inlet fuel filter. The fuel line consists of a close loop and an open discharge line to the spray facility. The closed loop consists of the supply tank, pump, pulsation dampener and the outlet filter. The pump is operated in the closed loop mode until the desired injection pressure is reached. Downstream of the pump exit a pulsation dampener is attached to reduce the pulsations to below 5%. The fuel is then passed through another filter to a three-way solenoid valve to switch the supply between the closed loop and the open discharge line. Upon reaching the desired injection pressure, fuel is supplied to the nozzle located inside the spray chamber by switching the supply from closed to open line using the solenoid valve. In this work, experiments are carried out at three injection pressures namely, 0.3MPa, 0.6MPa and 0.9MPa. The fuel injection pressure is measured using a pressure transducer (having a response time of 5ms and an accuracy of 0.13%) just upstream of the nozzle exit.

The spray chamber (having a dimension of 600mm (W) x 600mm (D) x 1200mm (H)) is made of a transparent, acrylic glass for optical measurements of which, two sides are detachable. The spray chamber is sealed from the outside environment operating with nitrogen gas supplied at a very flow rate from hood at the top to make the spray chamber ambient inert. Nitrogen gas supply hood and the nozzle exit have a clearance of about 350mm to ensure that the nitrogen supply does not affect the spray structure. The nitrogen, the liquid fuel and the fuel vapour are extracted continuously from the bottom using a collecting tray and an exhaust duct at the bottom in order to avoid vapour saturation inside the chamber.

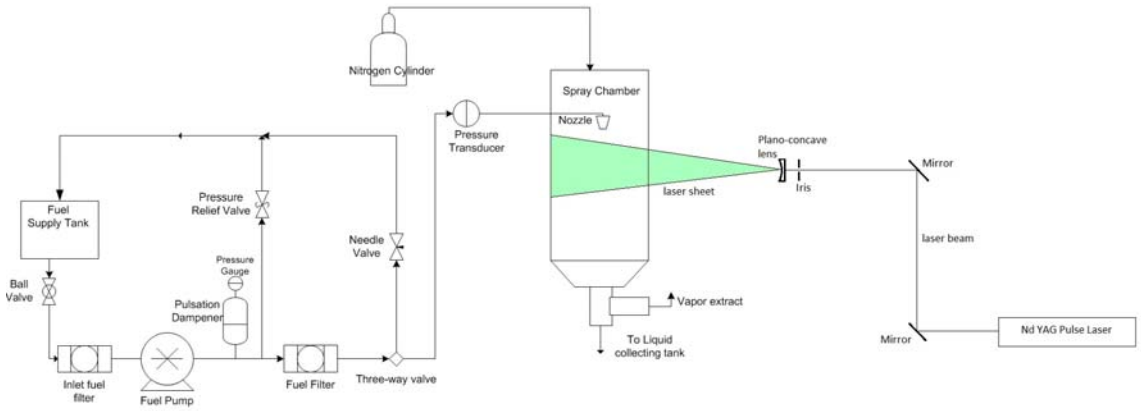

Figure 1 Optically accessible spray experimental facility

The optical module houses the required optics to properly guide and reform the laser beams used in this work. These optical devises include spherical and cylindrical lenses, mirrors pin-hole and traversing systems. Laser power meters are also placed on the module for detailed calibration of the systems. Inside the fuel chamber, the nozzle is mounted on a traversing mechanism to facilitate the movement of the field of investigation. The nozzle used in this work is a simple, pressure swirl nozzle with an exit diameter of 1.5mm provided by Rolls-Royce Plc, UK. The nozzle traverse opening is covered using a bellow. The region of interest downstream of the nozzle exit is divided in to five zones as shown in Fig. 2 where, each zone is 55mm x 41mm. In this work, only results pertaining to the nozzle location NS1-I and NS2-II alone are presented and discussed.

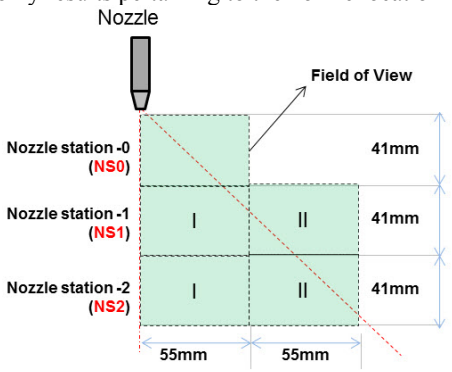

Figure 2 Experimental field of view

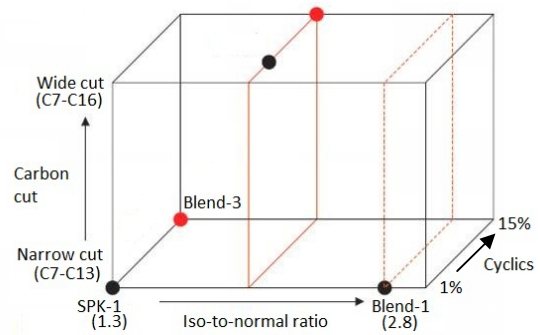

Figure 3 Fuel composition classifications [10]

Properties	Blend-1	SPK-1	Blend-3
Density (kg/m^3)	746.0	737.5	750.9
Viscosity (cSt)	3.27	2.552	2.985
H/C ratio	2.197	2.269	2.183
Iso-paraffins (% Wt)	73	56	48
Normal paraffins (% Wt)	26	43	37
Iso-to-normal paraffin ratio	2.8	1.3	1.3
Naphthenes (% Wt)	1	1	15

Table 1 GtL fuel and blend properties [10, 11]

The GtL-like fuel blends and Jet A-1 used in this work are supplied by Shell global solutions. The fuel characteristics are categorized based on iso-to-normal paraffin ratio, carbon range and the cyclic carbon content as shown in Fig. 3. For this study, the narrow carbon cut fuels namely, SPK-1, Blend-1 and Blend-3 are used to investigate the effects of iso-to-normal ratio and the cyclic carbon content on spray characteristics. The chemical composition and the fluid properties of GtL fuel and GtL-like blend are given in Table 1. The change in key fuel properties such as density and viscosity among the fuels are about 2% and 28% respectively. More details about the fuel preparation, properties and categorization are explained elsewhere [10].

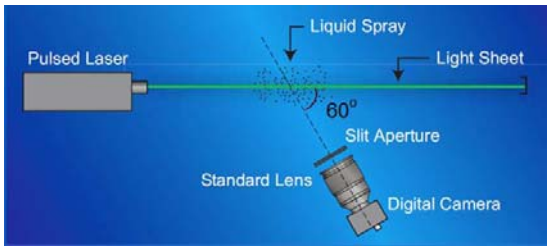

Figure 4 Laser-camera arrangement for GSV system [9]

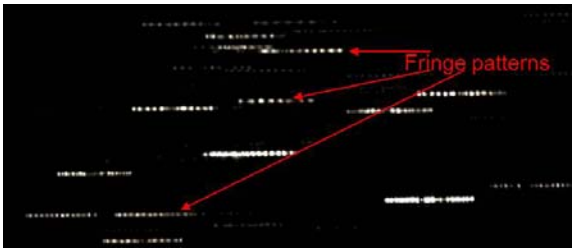

Figure 5 Sample fringe patterns

The droplet size and droplet velocity information are obtained using the Global Sizing Velocimetry (GSV) from TSI, Inc. [9]. Figure 4 shows the schematics of the laser-camera arrangement for the GSV technique. The

CCD camera is operated in a defocused mode and positioned at an angle of 60° to the laser sheet as, the oscillation spacing is most insensitive to refractive index at 60°[9]. Before the operation, the camera is focused on a calibration target to get the magnification factor then the camera is moved back to defocus and capture the out-of-focus [12] angular oscillations exhibited by the fuel droplets. A sample angular oscillation pattern obtained during the experiments is shown in Fig. 5. The spacing between the oscillations patterns are calculated to obtain the droplet size information using [9],

$$d = x * \lambda / \vartheta \quad (1)$$

where, d is the droplet diameter, x is a coefficient (1.129), λ is the wavelength and ϑ is the angular oscillation. Angular oscillation, ϑ is determined as,

$$\vartheta = M * \delta * \Delta z * n \quad (2)$$

where, M is the Magnification factor, δ is the pixel size, Δz is the camera defocus distance and n is the oscillation spacing. The droplet velocity information is determined from the droplet displacement obtained by tracking individual droplets between the image frames taken at a known time interval. The droplets are identified by matching the droplet size with neighbour droplets. The experiments are carried out using SPK-1, Blend-1, Blend-3 and Jet A-1 and the results are compared across each other in the next section.

Results and Discussion

In this section, droplet size distributions, mean droplet diameter and mean velocities are presented. In addition to that, a qualitative comparison of the spray structure is also presented. First, the effect of iso-to-normal paraffin ratio is compared followed by, the effect of cyclic carbon content.

Figure 6 shows the comparison of droplet size distributions at nozzle station1-I (NS1-I) for Blend-1, SPK-1 and Jet A-1 at three different injection pressures. Marching from top to down shows comparison of drop size distribution as the injection pressure increases for each fuel. Marching from left to right shows the effect of fuel composition on the size distribution. In each plot, red and blue lines are drawn to show the location of mean droplet diameter and the Sauter mean diameter (SMD) respectively. In all the cases, the change in mean diameters follows similar trend. The key difference between blend-1 and SPK-1 is the high iso-to-normal paraffin ratio in blend-1 when compared to SPK-1.

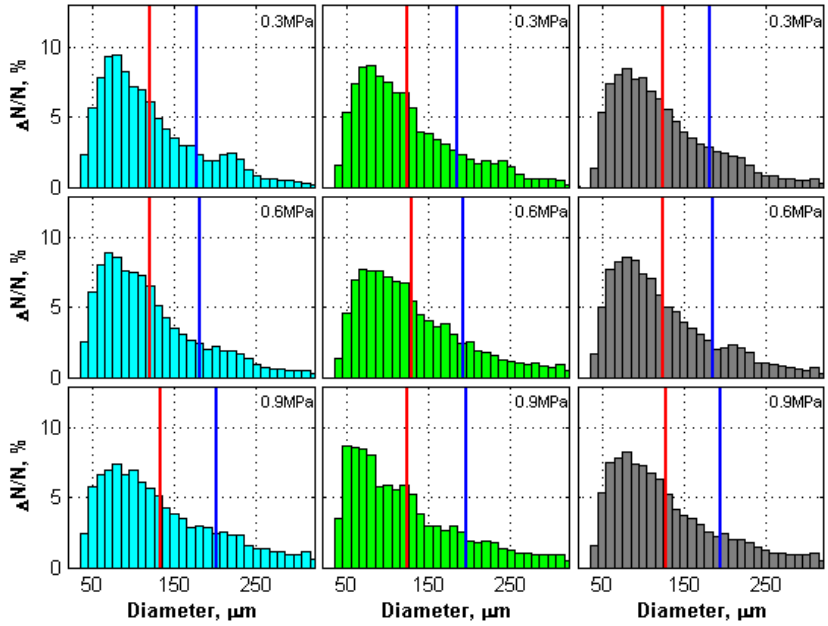

Figure 6 Droplet size distributions at NS1-I for Blend-1(left), SPK-1(middle) and Jet A-1 (right)

At low pressure, the mean droplet diameter is seen to shift towards higher range with the change in fuel composition. Blend-1 has lower mean droplet diameter when compared to SPK-1 and Jet A-1. Overall, the distribution has a similar trend for all the fuels at a given pressure. Figure 7 shows the comparison of the size distribution for fuels, blend-1, SPK-1 and Jet A-1 at nozzle location, NS2-II for different injection pressures. With the change in nozzle location from NS1-I to NS2-II, i.e., moving further downstream and radially outward from the nozzle exit, the size distribution exhibits a significant difference. The peak in the size distribution is seen to shift towards the lower droplet size and the percentage of droplets is seen to be higher when compared to NS1-I. In

addition, the droplet size distributions show a considerable difference between the fuels highlighting the effect of fuel composition on the size distribution. For Blend-1 with increase in injection pressure, the size distribution is seen to shift from higher to lower size side. However, the other two fuels show a completely opposite trend with increase in injection pressure. The difference in size distribution between blend-1 and Jet A-1 is significant when compared to the difference between SPK-1 and Jet A-1. This may be attributed to the influence of iso-to-normal paraffin ratio.

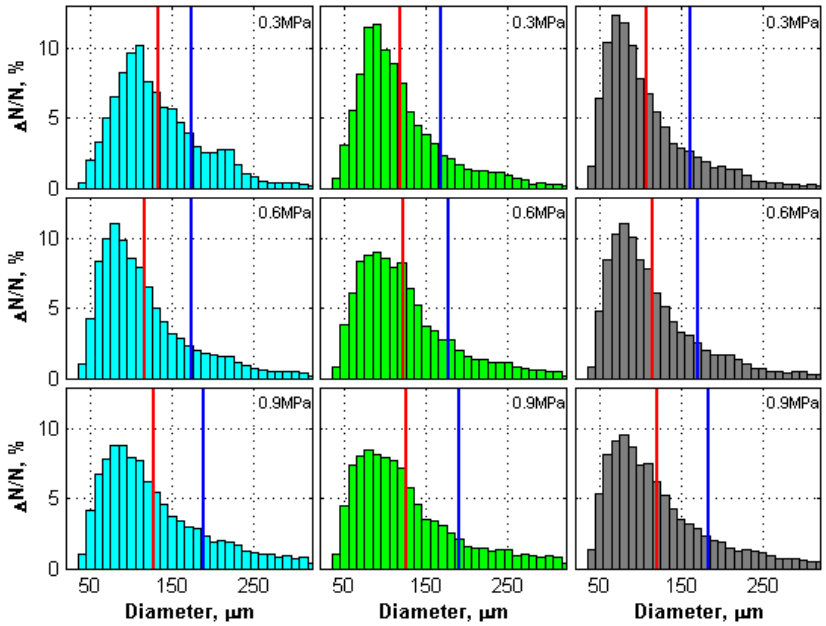

Figure 7 Droplet size distributions at NS2-II for Blend-1(left), SPK-1(middle) and Jet A-1 (right)

Figures 8 and 9 show the effect of cyclic carbon content on the droplet size distribution at nozzle locations, NS1-I and NS2-II respectively. The key difference between blend-3 and SPK-1is the high percentage of naphthene (with low carbon number range) in blend-3 when compared to SPK-1. In addition to this, blend-3 also has moderately high percentage of n-paraffins and iso-paraffins in the lower carbon numbers.

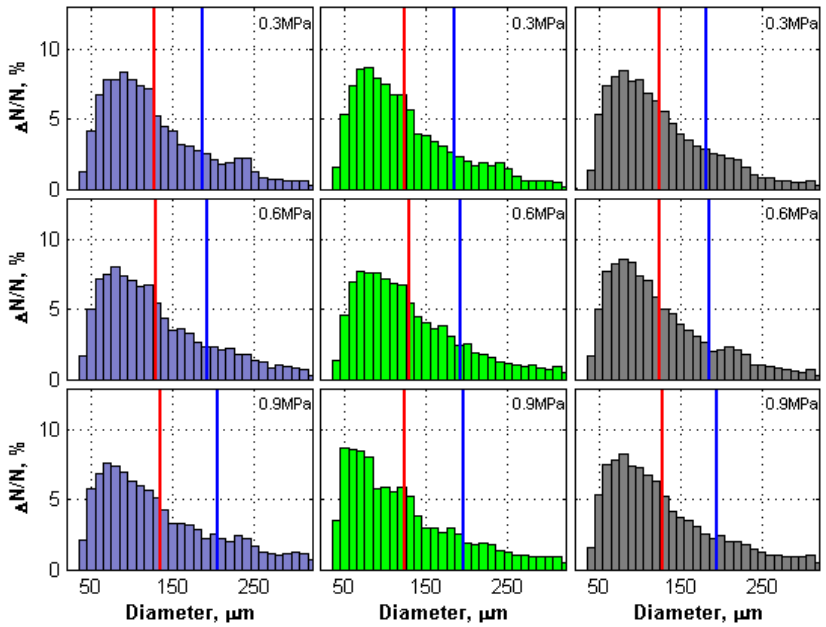

Figure 8 Droplet size distributions at NS1-I for Blend-3(left), SPK-1(middle) and Jet A-1 (right)

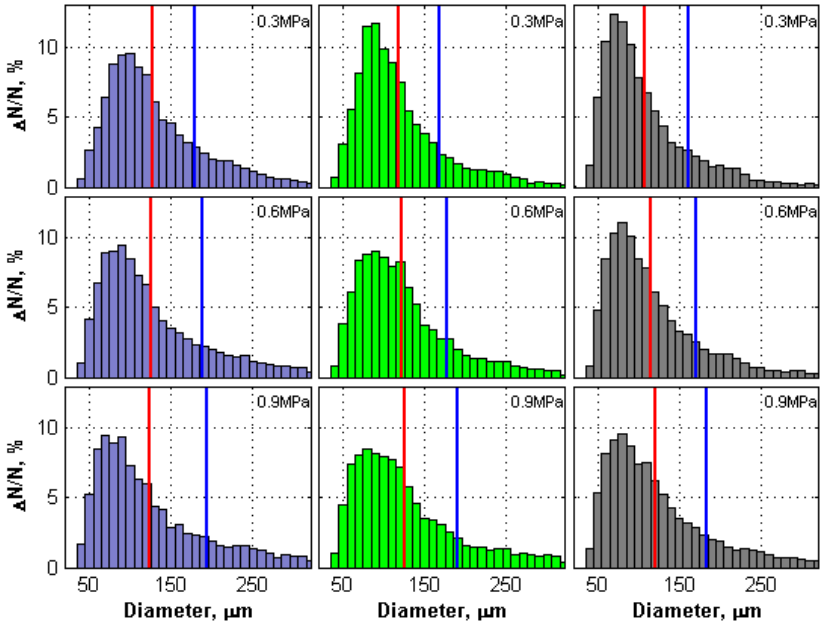

Figure 9 Droplet size distributions at NS2-II for Blend-3(left), SPK-1(middle) and Jet A-1 (right)

As in the case of iso-to-normal paraffin ratio, here also, the size distributions are found to be similar among the fuels at nozzle location, NS1-I. This suggests that very close to the nozzle exit, the effect of fuel composition have minimal effects. However, at a location further away from the nozzle exit, the size distributions show significant difference with change in injection pressure as well as fuel composition. At low injection pressure, blend-3 shows a broad distribution when compared to SPK-1 and Jet A-1 fuels. With increase in injection pressure, the peak distribution shifts toward smaller droplet size. This trend is very similar to the trend observed in Fig. 7. This in turn highlights the fact that the effect of increase in iso-to-normal paraffin ratio or the effect of increase in cyclic carbon content has similar effect on the droplet spray characteristics.

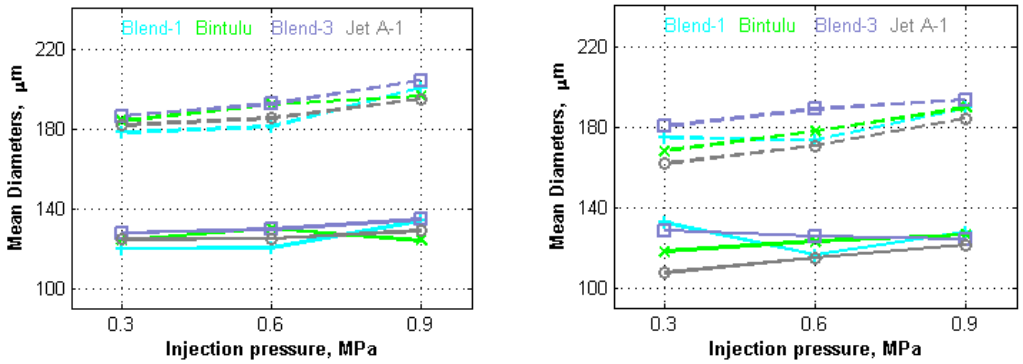

Figure 10 Mean droplet diameter variation at NS1-I (left) and NS2-II (right) for Blend-1, Blend-3, SPK-1 and Jet A-1

The variation of mean droplet diameters, mean and Sauter mean diameters, between the fuels at different injection pressures and nozzle locations are summarized in Fig. 10. The continuous line represents the mean droplet diameter and the dashed line represents the Sauter mean diameter. It is clearly seen that at nozzle location NS1-I, the variation is within the uncertainty of the measurement for both the mean diameters. While, at nozzle location NS2-II, the variation is seen to be significant. This is consistent with the trend that is observed in the size distribution. In addition, the increase in Sauter mean diameter with increase in injection pressure is an unexpected trend. However, the increasing trend is consistent among the fuels which in turn imply that it could be due to the measuring technique. The increasing trend could be due to the thickness of the laser sheet which results in detection of two or more smaller droplets separated by a small distance as one big droplet by the camera. Further

investigation is warranted to resolve this trend. The variation of mean velocity profiles at nozzle locations, NS1-I and NS2-II for blend-1, blend-3, SPK-1 and Jet A-1 at all injection pressures are shown in Fig. 11. At nozzle location, NS1-I, the velocity profiles show an increase in mean velocity with an increase in injection pressure. The mean velocities are seen to vary within 15% among the fuel blends. At nozzle location, NS2-II, except for blend-1, the mean velocity increases with an increase in injection pressure from 0.3MPa to 0.6MPa. However, the increase in injection pressure from 0.6MPa to 0.9MPa shows a mixed trend among the blends.

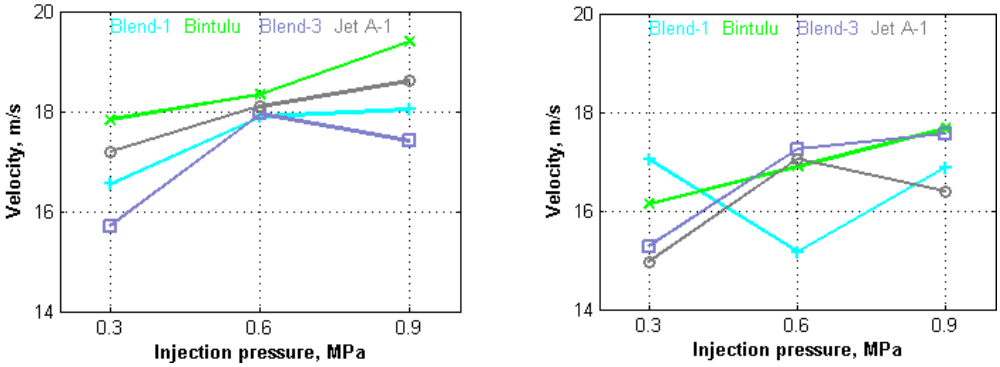

Figure 11 Mean velocity profiles at nozzle locations, NS1-I (left) and NS2-II (right) for Blend-1, Blend-3, SPK-1and Jet A-1

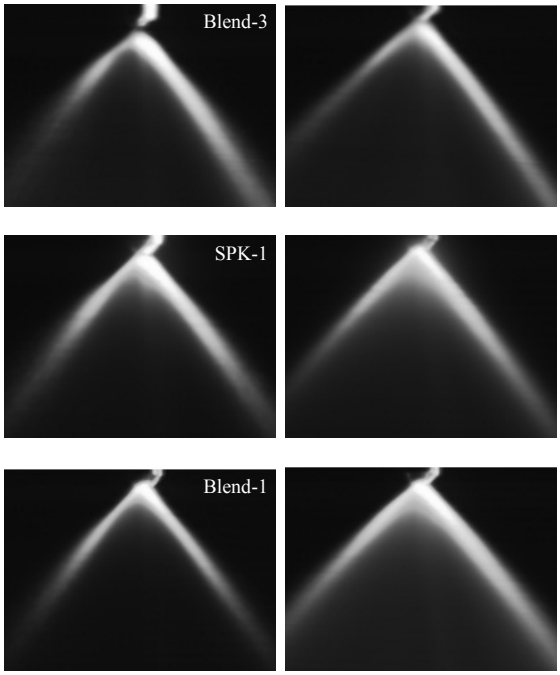

Figure 12 Spray cone structure for Blend-3(top), SPK-1(middle) and Blend-1 (Bottom) at 0.3MPa (left column) and 0.9MPa (right column) injection pressures

Figure 12 shows the qualitative change in the spray cone shape for three different GtL blends at injection pressures, 0.3MPa (left) and 0.9MPa (right). For all the cases, the laser power is maintained the same. The average spray cone structure shown in Fig. 12 is an average of 500 instantaneous images captured at a rate of 1000frames per second. In all the cases, it is evident that the spray cone angle increases with an increase in injection pressure from 0.3MPa to 0.9MPa as expected. Among the blends, blend-1 has the maximum brightness and blend-3 shows the least brightness. SPK-1 falls in between blend-1 and blend-3. This could be attributed to the change in fuel composition among the blends. Figure 12 seems to suggest that the change in iso-to-normal ratio is having profound effect when compared to the change in cyclic content of the fuel.

Summary and Conclusions

In this work, the influence of fuel chemical composition on the spray characteristics such as drop size, distribution, velocity and spray cone structure is investigated using three different GtL-like fuel blends and the conventional Jet A-1 fuel. Using a simplex nozzle, three injection pressures is studied in this work. The size and velocity measurements are carried out using an optical global sizing velocimetry technique.

The size distribution is measured at two nozzle locations, one close to the nozzle axis and the nozzle exit and one away from the nozzle exit and the nozzle axis. The results clearly show that at the location close to the nozzle exit and nozzle axis, the influence of iso-to-normal paraffin ratio and the cyclic carbon content is seen to be minimal. Similar trend is seen on the mean velocity profile in this location. While, at a location away from the nozzle axis and nozzle exit, the influence is seen to be significant for both iso-to-normal paraffin ratio and the cyclic carbon content. In addition, a qualitative inference is drawn from the spray cone structure that the iso-to-normal ratio has a profound effect when compared to the cyclic content.

Although the initial results seem to highlight the influence of chemical composition on the spray characteristics, further investigation is needed to draw definite conclusions on the effect of fuel composition on spray characteristics and it is underway.

Acknowledgements

This project is funded by Qatar Science and Technology Park (QSTP) under the contract A6730. Authors would like to thank and acknowledge the support extended by QSTP and all the project partners at Shell global solutions, Rolls-Royce Plc, UK, and DLR, Germany for their support.

References

[1] Le Clercq, P., Domenico, M. K., Rachner, M., Ivanova, E., and Aigner, M., *48th AIAA Aerospace Sciences Meeting*, Florida, 4-7 January, AIAA-2010-613, (2010).

[2] Kahandawala, M. S. P., DeWitt, M. J., Corporan, E., and Sidhu, S. S., *Energy & Fuels* 22:3673-3679 (2008).

[3] Gokulakrishnan, P., Klassen, M. S., and Roby, R. J., *Proc. of ASME Turbo Expo 2008: power for land, Sea and Air*, Berlin, 9-13 June, GT2008-51211, (2008).

[4] Corporan, E., DeWitt, M. J., Belovich, V., Pawlik, R., Lynch, A. C., Gord, J. R., Meyer, T. R., *Energy & Fuels* 21-5:2615-2626 (2007).

[5] Lefebvre, A. H., Atomization and Sprays, CRC Press, (2000).

[6] Yao, S., Zhang, J., and Fang, T., *ILASS America*, Ohio, May, (2010).

[7] Chrigui, M., Sadiki, A., Janicka, J., Hage, M., and Dreizler, A., *Atomization and sprays* 19-10: 929-955 (2009).

[8] Pucher, G., Allan, W., LaViolette, M., and Piotras, P., *Journal of Engineering for Gas Turbines and Power* 133:111502, (2011).

[9] Pan, G., Shakal, J., Lai, W., Calabria, R., Massoli, P., *ICLASS-2006*, Kyoto, Japan, Aug 27-Sep1, ICLASS06-283, (2010).

[10] Joanna M. Bauldreay, Paul F Bogers and Ali Al-Sharshani, *12th International conference on stability, handling and use of liquid fuels*, Florida, 16-20 October, (2010).

[11] Thomas Mosbach, Gregor C. Gebel, Patrick Le Clercq, Reza Sadr, Kumaran Kannaiyan, and Ali Al-Sharshani, *Proceedings of ASME Turbo Expo 2011: Power for Land, Sea and Air*, Vancouver, Canada, 6-10 June, GT2011-45510, (2011).

[12] Calabria, R., Casaburi, A., Massoli, P., *9th International Conference on Liquid Atomization and Spray Systems – ICLASS 2003*, Italy, 13-17 July, (2003).